The Oncologist®
Head and Neck Cancers

Cetuximab May Inhibit Tumor Growth and Angiogenesis Induced by Ionizing Radiation: A Preclinical Rationale for Maintenance Treatment After Radiotherapy

GEMMA PUEYO,[a] RICARD MESIA,[b] AGNES FIGUERAS,[a] ALICIA LOZANO,[c] MARTA BARO,[a] SILVIA VAZQUEZ,[b] GABRIEL CAPELLA,[a] JOSEP BALART[a,d]

[a]Translational Research Laboratory, IDIBELL, on behalf of Program of Applied Radiobiology of Catalonia (PRACAT), [b]Medical Oncology Department and [c]Radiation Oncology Department, Catalan Institute of Oncology, L'Hospitalet de Llobregat, Spain; [d]Radiation Oncology Department, Hospital de la Santa Creu i Sant Pau, Barcelona, Spain

Key Words. Cetuximab • Radiotherapy • Maintenance therapy • EGFR • Angiogenesis • Cytoprotection

Disclosures: Gemma Pueyo: *Research funding/contracted research:* Merck Serono; **Ricard Mesia:** *Honoraria:* Merck Serono; **Agnes Figueras:** None; **Alicia Lozano:** None; **Marta Baro:** None; **Silvia Vazquez:** None; **Gabriel Capella:** None; **Josep Balart:** None.

The article discuss the unlabeled, investigational, or alternative use of the monoclonal antibody cetuximab (Merck Serono) as maintenance treatment after radiotherapy.

The content of this article has been reviewed by independent peer reviewers to ensure that it is balanced, objective, and free from commercial bias. No financial relationships relevant to the content of this article have been disclosed by the independent peer reviewers.

ABSTRACT

Background. **The benefits of radiotherapy and cetuximab have encouraged evaluation of cetuximab after radiotherapy. The aims of this study were to preclinically evaluate the efficacy of cetuximab maintenance after radiotherapy and eventually determine its mechanisms of action.**

Methods. **The A431 human carcinoma cell line was treated in culture with fractionated radiotherapy and cetuximab. The surviving cells were injected s.c. into nude mice to mimic microscopic residual disease. The animals were randomized to receive either cetuximab or saline solution. Tumor growth, cell proliferation (Ki-67), microvessel density (MVD), epidermal growth factor receptor (EGFR) and transforming growth factor (TGF-α) mRNA transcription, and vascular endothelial growth factor (VEGF) secretion were measured.**

Results. **Tumors from irradiated cells had a faster growth rate, higher Ki-67 index, and greater angiogenesis than tumors from untreated cells. This aggressive phenotype was associated with in vitro radiation-induced extracellular signal–related kinase (ERK)-1/2 and Akt activation, greater EGFR and TGF-α transcription, and augmented VEGF secretion, all of which were inhibited by cetuximab. In cetuximab-treated mice with tumors arising from irradiated cells, time to volume was longer by a factor of 3.52, whereas the Ki-67 index and MVD were 1.57 and 1.49 times lower, respectively, a larger enhancement than seen in tumors from untreated cells. These findings suggest that cells surviving radiation may express factors that promote cell survival and induce an aggressive**

Correspondence: Josep Balart, M.D., Ph.D., Laboratori de Recerca Translacional-IDIBELL, Institut Català d'Oncologia, Hospital Duran i Reynals, Avda Gran Via de l'Hospitalet, 197–203, L'Hospitalet de Llobregat 08907, Spain. Telephone: 34-93260-7952; Fax: 34-93260-7644; e-mail:jbalart@iconcologia.net Received December 24, 2008; accepted for publication June 23, 2010; first published online in ***The Oncologist*** *Express* on August 26, 2010. ©AlphaMed Press 1083-7159/2010/$30.00/0 doi: 10.1634/theoncologist.2008-0290

phenotype that may potentially be blocked by cetuximab maintenance therapy.

Conclusions. **These results support the clinical evaluation of adjuvant therapy with cetuximab after radiotherapy in EGFR-dependent carcinomas.** ***The Oncologist*** 2010;15:976–986

INTRODUCTION

Advances in the field of imaging diagnosis together with new methods of radiation delivery have substantially increased the curative potential of radiation oncology. However, despite these technological improvements, recurrence after radiotherapy is still a major cause of death in patients with locally advanced disease.

Recurrences are believed to be caused by the small fraction of cancer cells (subclinical or microscopic residual disease) that retain their clonogenic capacity after radiotherapy. Recently, some authors have hypothesized that such cells may actually be cancer stem cells that—in addition to self-renewal and cancer cell multilineage growth—exhibit an intrinsic radioresistance attributable to hypoxia adaptability, elevated tumor-associated angiogenesis, high efficiency in repairing radiation-induced DNA damage, and accelerated tumor repopulation [1–4].

Cancer stem cell radioresistance has been associated with cellular pathways that promote cell survival, among which is the epidermal growth factor receptor (EGFR) signaling pathway [5]. Abnormal EGFR hyperactivity may lead to the upregulation of several oncoproteins, such as Ras and phosphatidylinositol 3-kinase, both of which play a central role in tumor progression, including angiogenesis and metastatic dissemination [6]. EGFR overexpression is associated with aberrant survival, resistance to radiotherapy and chemotherapy, and poor prognosis in many cancers [7], and therefore represents a potential target for cancer therapy.

Cetuximab is a chimeric human–mouse antibody that binds specifically to human EGFR (EGFR/HER-1) with greater affinity than EGFR natural ligands—in particular, transforming growth factor (TGF-α)—thereby blocking receptor activation. Cetuximab has been found to have an antitumorigenic effect when added to radiotherapy in the treatment of locally advanced head and neck squamous cell carcinomas (HNSCCs), in which EGFR overexpression is highly frequent. Treatment with cetuximab has led to significantly longer overall survival times, with a survival rate similar to that achieved by concomitant chemoradiotherapy, but with less toxicity [8].

The ongoing success of radiotherapy and cetuximab has fueled interest in cetuximab as a potential adjuvant treatment following radiotherapy [8–10]. The rationale for this emerging indication is that cetuximab would not only increase cell radiosensitivity during radiotherapy but may also continue to inhibit the proliferation of residual clonogenic cells after radiotherapy. The main objective of this study was to assess the effects of cetuximab in a mouse model on tumors derived from a subpopulation of previously irradiated cells.

In our model, we found that the subpopulation of cells that survived radiation displayed an aggressive tumor phenotype associated with greater EGFR pathway activation. In addition, cetuximab actually inhibited tumor progression despite the malignant growth characteristics of tumors derived from irradiated cells.

MATERIALS AND METHODS

Cell Culture and In Vitro Cell Pretreatment

The human epidermoid carcinoma cell line A431, which overexpresses EGFR, was used. Cells were maintained in culture as a monolayer in a humidified incubator at 37°C in 5% CO_2 atmosphere and irradiated at room temperature (RT) at a dose rate of 2.7 Gy/minute with 6 MV x-rays from a linear accelerator. Cetuximab (30 nmol/l; Merck KGaA, Darmstadt, Germany) was added to the culture medium and renewed every 3.5 days. Radiation and cetuximab were administered according to the treatment schedules shown in Figure 1. In 145-cm^2 dishes, 2×10^6 A431 cells were plated and allowed to grow as a confluent culture. The cell monolayer was not harvested until the end of treatment, at which time plating—to measure residual colony formation capacity—and injection into mice took place. The effect of cetuximab on colony formation was assessed. A standard clonogenic assay on plastic dishes was undertaken to determine the survival fraction (SF) of cells after in vitro treatment. SF was calculated as the ratio between colony formation following treatment and colony formation by untreated cells.

Mice and Tumor Model

All experimental procedures were approved in accordance with our own institutional guidelines for animal care and ethics. Six- to 8-week-old male athymic Swiss nu/nu mice were purchased from Harlan (Gannat, France) and housed under pathogen-free conditions at our facilities (Association for Assessment and Accreditation of Laboratory Animal Care accreditation number 1155). Tumors were

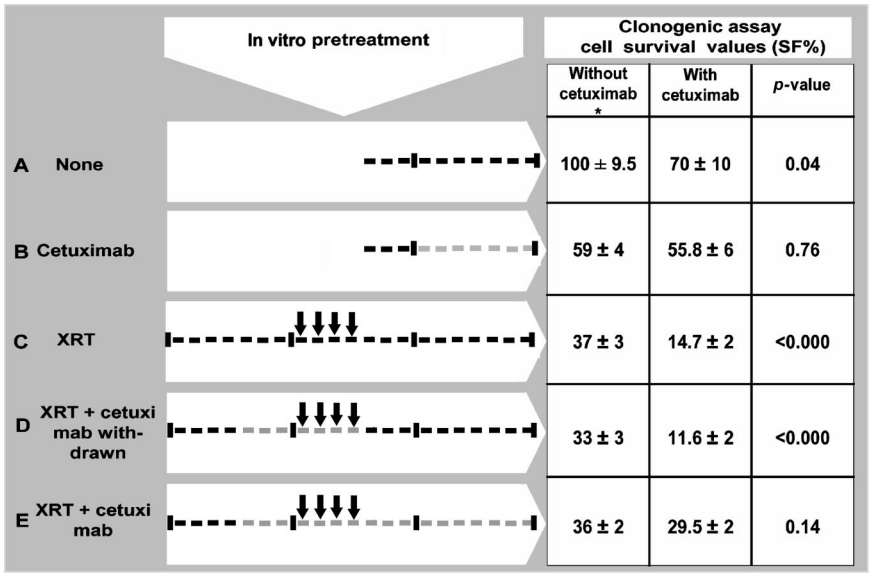

Figure 1. Cells were cultured for 3 weeks, represented here by three segments divided into 7 days (hyphens). Arrows indicate 2 Gy of radiation (XRT), and the gray lines indicate cetuximab exposure. The surviving fraction (SF) is given in the absence or presence of cetuximab during colony formation.

*Values used to adjust the number of cells injected.

generated through s.c. cell injection into the right flank. Injected cells were obtained from cell cultures treated in vitro (Fig. 1). Mice were randomized to receive either saline solution or 0.1 mg of cetuximab i.p. (0.45 ml) 3.5 days before tumor cell injection and 0.05 mg/mouse at intervals of 3.5 days thereafter until sacrifice. The mice received no radiation treatment. Tumor size was calculated according to the formula $\pi/6 \times$ large diameter $\times$ small diameter^2. To measure tumor latency and progression, tumor growth was monitored and the actuarial mean time to reach a given volume was recorded as the endpoint. The mice were euthanized when tumor volume reached 1,000 mm^3.

Determination of Ki-67$^+$, CD31$^+$, and F4/80$^+$ Cells by Immunostaining

Tumor cell proliferation was estimated by immunofluorescence staining of the Ki-67 antigen. Cryostat sections (3-μm thick) of xenografted tumors embedded in OCT compound (Sakura Finetek Europe, Zoeterwoudl, The Netherlands) were fixed with 10% neutral-buffered formaldehyde. The samples were washed (0.1% Triton in phosphate-buffered saline [PBS]) and incubated for 1 hour at RT with protein-blocking solution (PBS containing 20% normal goat–horse serum). Next, the slices were incubated for 30 minutes with mouse anti-Ki-67 primary antibody (NeoMarkers, Fremont, CA) at a dilution of 1:100 followed by incubation with AlexaFluor 594–conjugated goat anti-mouse secondary antibody (Invitrogen, Carlsbad, CA) at a dilution of 1:200 for 1 hour, all at RT. Then, slices were mounted using Vectashield mounting medium with 4′,6-diamidino-2-phenylindole (Vector Laboratories Inc., Burlingame, CA). Fluorescence images were captured using a Zeiss Axioplan 2 imaging epifluorescence microscope equipped with a charge-coupled device camera and SPOT advanced software (Diagnostic Instruments, Inc., Sterling Heights, MI). Five randomly selected field microscopic images (magnification, 40×) per slice were analyzed. The Ki-67 index was calculated based on counting positive nuclei in a minimum of 2,000 cells per treatment condition from three independent tumors. Cells were counted using the ImageJ program, public domain Java image-processing software (http://rsb.info.nih.gov/ij/).

Angiogenesis and macrophage infiltration were assessed by determination of the CD31 (platelet and endothelial cell adhesion molecule 1) endothelial marker and macrophage-specific F4/80 antigen, respectively. Briefly, cryostat sections (3-μm thick) of xenografted tumors embedded in OCT compound were fixed with 10% neutral-buffered formaldehyde. Endogenous peroxidases were blocked with 3% H_2O_2 in PBS. The samples were washed (0.1% Triton in PBS) and incubated for 1 hour at RT with protein-blocking solution (PBS containing 20% normal goat–horse serum). Next, they were incubated either with a rat anti-CD31 monoclonal antibody (Becton Dickinson Immunocytometry Systems, San Jose, CA) or with rat anti-mouse F4/80 antigen monoclonal antibody (AbD Serotec, Dusseldorf, Germany), both at a 1:50 dilution for 30 min-

utes at RT. Then, the slides were treated for 30 minutes with rabbit anti-rat biotinylated IgG at a 1:200 dilution at RT, incubated with 3.3′-diaminobenzidine chromogen (Dako-Cytomation, Glostrup, Denmark), counterstained with hematoxylin, and mounted with mounting medium after dehydration with alcohol and xylene. Microvessel density (MVD) was determined by light microscopy after frozen sections were immunostained with anti-CD31 antibody. This method has been described in depth elsewhere [11]. Briefly, areas containing the highest number of capillaries were identified at low power magnification (10×), and then five 40× fields per slice were examined for MVD count in a blinded fashion. MVD was calculated based on counting 45 fields per treatment condition (nine tumors) from three independent experiments. Macrophage infiltration was scored using the same approach as for MVD count.

Phosphorylated ERK-1/2 and Phosphorylated Akt Immunoblotting

Cell cultures were maintained without fetal bovine serum (FBS) for 24 hours before treatment with EGF (Invitrogen), radiation, or cetuximab. Fifteen minutes following treatment, cells were rinsed in ice-cold PBS and lysed in RIPA lysis buffer for 10 minutes. Insoluble material was removed by centrifugation at 12,000 ×g for 5 minutes at 4°C. Protein concentration in the lysates was determined by the Pierce BCA Protein Assay Kit (Thermo Scientific, Rockford, IL). Equal amounts of protein (30 μg) were heated to 95°C for 5 minutes, resolved by 8% SDS-PAGE and blotted onto a nitrocellulose membrane (GE Healthcare – Amersham Pharmacia Biotech, Buckinghamshire, U.K.). After blocking with 5% nonfat dry milk in Tris-buffered saline for 1 hour, membranes were incubated with a mouse anti–mitogen-activated protein kinase (MAPK)-activated ERK-1/2 monoclonal antibody (Sigma-Aldrich, St. Louis, MO) at a dilution of 1:10,000, a rabbit anti–phosphorylated Akt (anti-pAkt) (Ser473) polyclonal antibody (Cell Signaling, Danvers, MA) at a dilution of 1:500, or a mouse anti-tubulin monoclonal antibody (Sigma-Aldrich) at a dilution of 1:5,000 in blocking solution overnight at 4°C. Next, membranes were washed and incubated with anti-mouse IgG or anti-rabbit IgG horseradish peroxidase–linked antibody (GE Healthcare – Amersham Pharmacia Biotech) both for 1 hour at a dilution of 1:5,000. The blots were developed using the enhanced chemoluminescence staining ECL™ western blotting system (GE Healthcare – Amersham Pharmacia Biotech).

Quantitative Real-Time Polymerase Chain Reaction Expression of EGFR and TGF-α

Total RNA was isolated from cell cultures and xenografts using Trizol reagent (Invitrogen) followed by precipitation in isopropyl alcohol. Quality of the RNA was confirmed by electrophoresis on 1% agarose gel containing ethidium bromide. Total RNA was reverse transcribed using anchored-oligo-(dT)20 primers and the transcriptor first strand cDNA synthesis Kit (Roche Applied Science, Penzberg, Germany) according to the package inserts. AMV retrotranscriptase was inactivated by incubating samples for 5 minutes at 95°C. Then, cDNA was amplified using a LightCycler 480 instrument (Roche). The primers used were designed to amplify human-specific sequences. For EGFR, primer sequences (5′→3′) were as follows: forward primer, TAA AAC CGG ACT GAA GGA G; reverse primer, ACT GCT GAC TAT GTC CCG. For TGF-α they were: forward primer, GAC AGC TCG CCC TGT TC; reverse primer, CTG GGC AGT CAT TAA AAT GG. To account for potential variation in RNA, the expression levels of EGFR and TGF-α were normalized to endogenous human glyceraldehyde-3-phosphate dehydrogenase (GAPDH). For this gene, the forward primer was CTC CAC CTT TGA CGC T and the reverse primer was CTC CAC CTT TGA CGC T. The sizes of polymerase chain reaction (PCR) products were 130 bp for EGFR, 129 bp for TGF-α, and 93 bp for GAPDH. In order to quantify the number of EGFR, TGF-α, and GAPDH mRNA copies, standard (calibration) curves were generated from serial dilution of the former specific PCR products cloned into pCR4-TOPO vector (Invitrogen).

VEGF Determination

In 21-cm^2 dishes, 4 million A431 cells were plated and allowed to grow with 0.5% FBS for 24 hours. Supernatants were collected from semiconfluent cultures at increasing time points afterwards. Vascular endothelial growth factor A (VEGF), the most relevant mitogenic factor for endothelial cells, was evaluated by enzyme-linked immunosorbent assay (R & D Systems Inc, Minneapolis, MN). A standard curve following the manufacturer's instructions was generated for each experiment assay. To calculate VEGF concentration in supernatants, we used regression analysis from the standard curve with VEGF values normalized by cell counting.

Statistical Analysis

Results are expressed as mean ± standard error (SE). The Statistical Package for Social Sciences (SPSS, version 13.0; SPSS, Inc., Chicago, IL) was used for data analysis. Statistically significant differences in between-group comparisons were defined using a two-tailed significance level of $p < .05$ in statistical tests.

Table 1. Days to reach 100 mm^3 tumor volume as a function of treatment

	In vivo treatment			
In vitro pre-treatment	**Saline**	**Cetuximab**	***p*-value**	**Factor**
None (A)	7.9 ± 1.6	14.3 ± 1.7	.001	1.81
30 nM cetuximab alone (B)	5.6 ± 0.4	15.2 ± 3.6	<.001	2.71
XRT alone (C)	4.8 ± 0.35[a]	16.9 ± 2.8	<.001	3.52
XRT + cetuximab withdrawn (D)	5.0 ± 0.3[a]	11.3 ± 1.1	< .001	2.26
XRT + cetuximab (E)	4.6 ± 0.4[a]	13.9 ± 1.6	<.001	3.02

Days to reach 100 mm^3 are shown as mean ± standard error of six independent experiments with three mice per experiment.
[a]$p < .05$ versus tumors derived from untreated cells (Mann-Whitney test).
Abbreviation: XRT, radiation.

RESULTS

In Vitro Pretreatment

A431 cells growing as a confluent monolayer culture were sublethally irradiated with 4 doses of 2 Gy (schedule C) administered every 24 hours and kept in the same dishes for 2 weeks before the clonogenic assay (Fig. 1). Although most cells displayed progressive changes compatible with radiation damage (giant cell formation, large nuclei, and cytoplasmic vacuolization), a portion remained resistant to the radiation, as evidenced by the fact that they continued to grow as a monolayer while retaining their colony-forming capacity. Surviving cells were allowed to repopulate whereas radiation-killed cells were removed by periodic growth medium renewal. The remaining attached cells yielded an SF of 37% (Fig. 1). Preliminary experiments showed that higher doses of radiation severely diminished cell culture viability, precluding the implementation of additional experiments.

Because cetuximab is usually added concomitantly to radiation in the treatment of patients with advanced malignancies such as HNSCCs, we examined the effects of both agents in vitro on A431 cells. The addition of cetuximab to radiation (schedules D and E) did not lead to a further reduction in cell survival (Fig. 1). The lack of effect on the SF may have been a result of a transitory cell adaptation process or permanent resistance to cetuximab [12, 13]. To test for an adaptive response in our model, cells were given additional treatment with cetuximab during colony formation. In that setting, cetuximab led to a significantly lower SF after radiation alone (schedule C), 15% versus 37%, demonstrating the benefit of adding an anti-EGFR treatment to irradiated A431 cells. In contrast, no significant reductions in cell survival were observed with maintenance treatment (schedules B and E). Interestingly, those cells that had become insensitive to cetuximab treatment regained sensitivity after treatment was withdrawn (schedule D) (Fig. 1). These facts suggest that the observed resistance to cetuximab was transient and reversible.

Cetuximab May Have Preferentially Inhibited the Growth of Tumors Derived from Cells That Survived In Vitro Irradiation

A431 cells were injected into mice to evaluate the effects of cetuximab on tumors originating from cells treated in vitro according to the schedule shown in Figure 1. The injection of 1 million untreated A431 cells in 100 μl gave rise to a tumor in 97% of the experimental mice, with progressive growth following injection. The mean cloning efficiency of untreated A431 cells was consistent with the presence of 95,000 clonogenic cells per million. In order to evaluate the efficacy of in vivo cetuximab, this clonogenic burden was kept constant by adjusting the total number of injected cells as a function of in vitro SF values (Fig. 1), which varied depending on the in vitro treatment schedule. However, animals treated according to the same in vitro schedule were injected with an identical number of cells.

In contrast with the in vitro findings, in vivo maintenance treatment with cetuximab had a notable negative impact on tumor growth (Table 1). To explore whether the antitumor effect of cetuximab was mediated by antibody-dependent cellular cytotoxicity (ADCC), we determined macrophage infiltration into xenograted tumors. Although macrophage-mediated ADCC has been reported in therapy using monoclonal antibodies [14], in this model, treatment with in vivo cetuximab was not followed by an accumulation of $F4/80^+$ cells at the tumor site (supplemental online Fig. S1), suggesting that the immune response was not relevant to the action of cetuximab in our model system.

Treatment with in vivo cetuximab inhibited the growth of xenografts with enhancement factors similar to those in previous reports [15]. In mice injected with untreated cells (schedule A), the time for a tumor to reach 100 mm^3 was 7.9 days in saline-treated animals and 14.3 days in cetuximab-

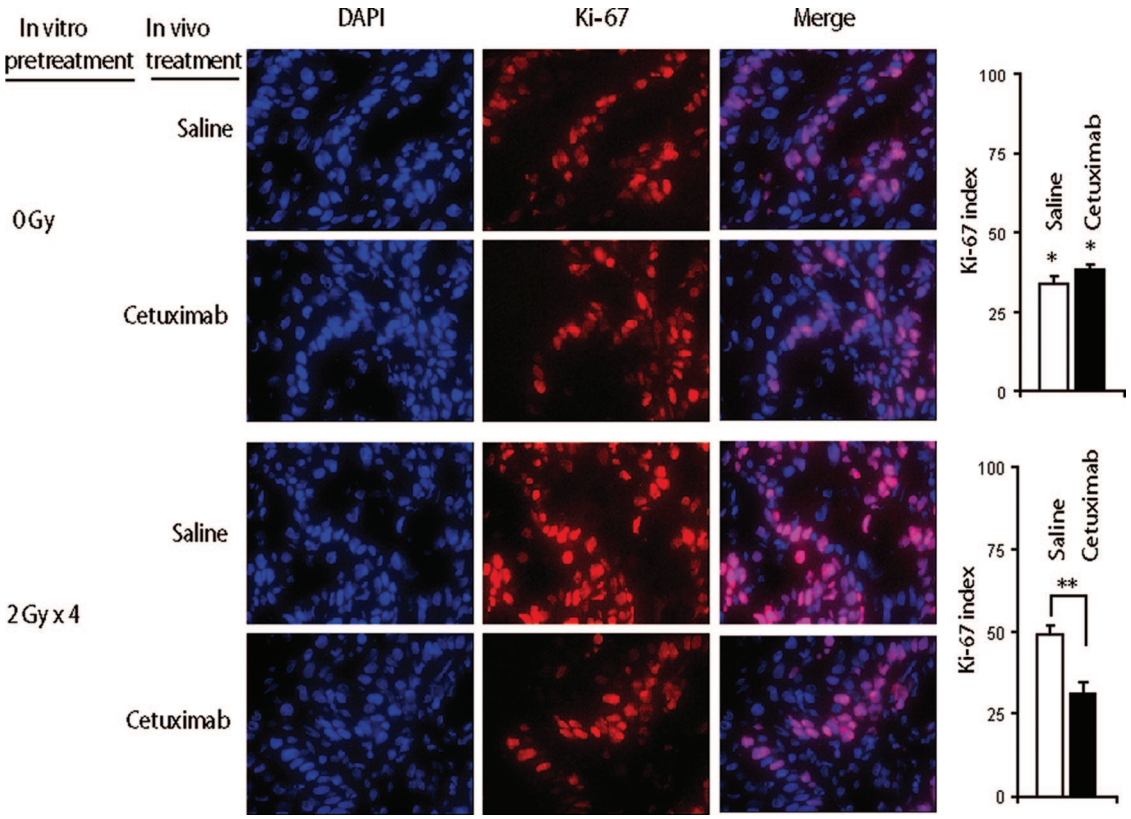

Figure 2. Cetuximab preferentially inhibited cell proliferation in tumors arising from in vitro–irradiated A431 cells. Representative Ki-67 immunostainings (40×) of xenografted tumors are depicted.

*$p = .01$, compared with tumors derived from irradiated cells in saline-treated and cetuximab-treated mice, respectively; **$p < .001$ (Student's t-test).

Abbreviation: DAPI, 4′,6-diamidino-2-phenylindole.

treated mice, 1.8 times greater (Table 1). In tumors derived from irradiated cells (schedule C), the elapsed time was significantly shorter (4.8 days) in saline-treated mice, indicating that ionizing radiation had induced accelerated growth. Interestingly, in these tumors, cetuximab was also effective at increasing the time elapsed to 16.9 days, 3.52 times greater (Table 1). These differences were maintained throughout the tumor growth (supplemental online Fig. S2). Notably, although cetuximab inhibited tumor growth in all experimental settings, we observed a nonsignificant trend toward a higher efficacy in tumors derived from cells pretreated with radiation alone ($p = .12$; analysis of variance test).

We next explored whether variations in tumor growth were actually related to differences in the cell growth fraction. Ki-67 antigen immunostaining was used. Histological examination showed non-necrotic, well-differentiated, squamous cell tumors in both nontreated and treated animals (data not shown). Tumors generated from untreated cells showed a lower Ki-67 index (33.74% ± 2.33%) than tumors derived from irradiated cells (49.34% ± 1.81%) (Fig. 2). The high Ki-67 value is consistent with accelerated growth of tumors from irradiated cells (Table 1). Treatment with in vivo cetuximab was associated with a lower Ki-67 index (31.4% ± 2.23%, versus 49.34% ± 1.81%), whereas no difference was observed in tumors from untreated cells (33.74% ± 2.33% versus 38.5% ± 1.58%), as illustrated in Figure 2. The vigorous response seen in xenografts derived from irradiated cells treated with cetuximab suggests that these tumors were highly dependent on EGFR signaling. On the other hand, in tumors derived from untreated cells, the dependency on EGFR inhibition was apparently lower, as evidenced by a smaller reduction in tumor growth after cetuximab treatment that was not associated with differences in Ki-67 immunostaining.

Ionizing Radiation Induced a Cytoprotective Response Before Implantation Into Mice

We hypothesized that ionizing radiation might have induced changes in the cell biology of A431 cells, leading to a more aggressive phenotype. The strong effect of cetuximab on these xenografts led us to examine whether EGFR signaling pathway activation was responsible for the observed phenotype. Thus, we explored whether A431 cells

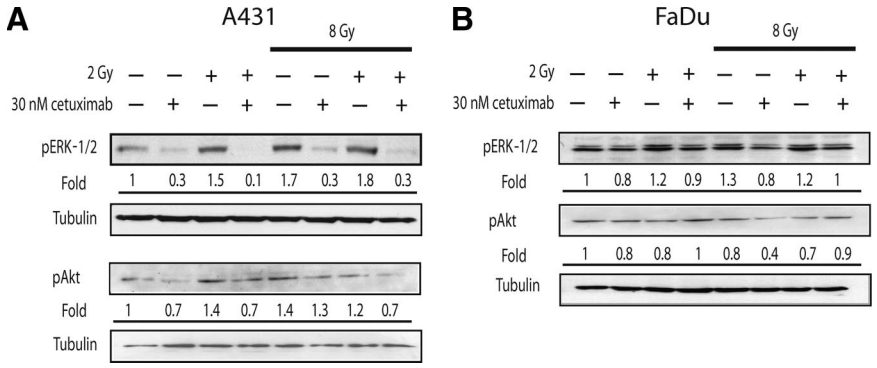

Figure 3. ERK-1/2 and pAkt activation were maintained during fractionated irradiation. A431 or FaDu cells were incubated for 24 hours to recover from 8 Gy of irradiation before an additional 2 Gy. Cetuximab was added 2 hours before cell lysis. Tubulin was included as a loading control. Densitometry values are indicated as fold relative to untreated cells.

Abbreviation: pERK-1/2, phosphorylated extracellular signal–related kinase.

responded to radiation by stimulating mechanisms involved in cell proliferation. As expected, unirradiated cells reacted to an EGF stimulus (2.5 ng/ml × 10 minutes) by increasing MAPK ERK-1/2 levels, a response that was inhibited by cetuximab (data not shown). In addition to EGF, a 2-Gy dose of ionizing radiation also induced an increase in pERK-1/2 levels, and after exposure to 8 Gy, the activation of ERK-1/2 was maintained for at least 24 hours (Fig. 3A). Importantly, blocking EGFR specifically using cetuximab diminished signaling induced by radiation. To examine whether other signaling molecules under the control of EGFR were also influenced by radiation therapy, we determined the levels of pAkt. We found that ionizing radiation induced the phosphorylation of Akt in a manner similar to pERK-l/2 (Fig. 3A). Moreover, the activation of Akt was partially inhibited by cetuximab, especially when the antibody was administered together with radiation. These findings indicate that EGFR is involved in the radiation-induced activation of these two major EGFR downstream signaling molecules, and suggest that the surviving (resistant) cells in this cellular model have an activated EGFR pathway.

To elucidate whether other cells could elicit a similar response to ionizing radiation we studied the FaDu cell line (American Type Culture Collection, Manassas, VA), which is derived from a human hypopharyngeal squamous carcinoma. FaDu cells show a moderate EGFR expression level, compared with A431 cells [16]. Similar to A431 cells, higher levels of pERK-1/2 following radiation therapy and inhibition of radiation-induced pERK signaling by cetuximab were observed (Fig. 3B). In contrast, the Akt level was not augmented after ionizing radiation (Fig. 3B), suggesting that, in FaDu cells, growth after radiation therapy relies on ERK-1/2 rather than the Akt pathway. The diminution of the phosphorylation of ERK-1/2 by blocking EGFR corroborates the idea that EGFR was intimately connected to mechanisms driving cell proliferation after ionizing radiation in the A431 and FaDu cell lines.

We then determined the levels of expression of EGFR and TGF-α, the main ligand of EGFR secreted by tumor cells. After radiation exposure, in vitro surviving A431 cells showed significantly higher (three times greater) EGFR levels than unirradiated cells (Fig. 4A). Similarly, TGF-α was overexpressed in irradiated cells, although these differences were not statistically significant (Fig. 4B). In vitro exposure to cetuximab was associated with significantly lower expression levels of both EGFR and TGF-α than with exposure to irradiation alone. In vivo, the expression levels of both genes were higher in tumors derived from irradiated cells than in tumors originating from untreated cells (Fig. 5). The addition of cetuximab treatment resulted in lower EGFR and TGF-α mRNA levels.

The previously reported effect of the EGFR signaling pathway on tumor-associated angiogenesis [17] and the upregulation of this pathway by radiation led us to investigate whether the angiogenic ability of the A431 cells was modified in our model system. In relatively small tumors (175.97 mm^3 ± 6.91 mm^3), the xenografts from cells treated with radiation alone (schedule C) that had the highest EGFR levels showed the highest MVD values, in stark contrast to tumors from unirradiated cells (Fig. 6 and supplemental online Table S1). Interestingly, cetuximab resulted in 1.49 times lower MVD values (supplemental online Table S1). Similar results were found in xenografted tumors treated according to schedule D (in vitro withdrawal of cetuximab), suggesting once more that the strong inhibitory effects observed may be a subsequent result of in vivo blocking of EGFR in previously radiation-stimulated cells. Indeed, inhibition of tumor-associated angiogenesis was less apparent in tumors treated according to schedules A, B, and E (supplemental online Table S1); tumors arising from

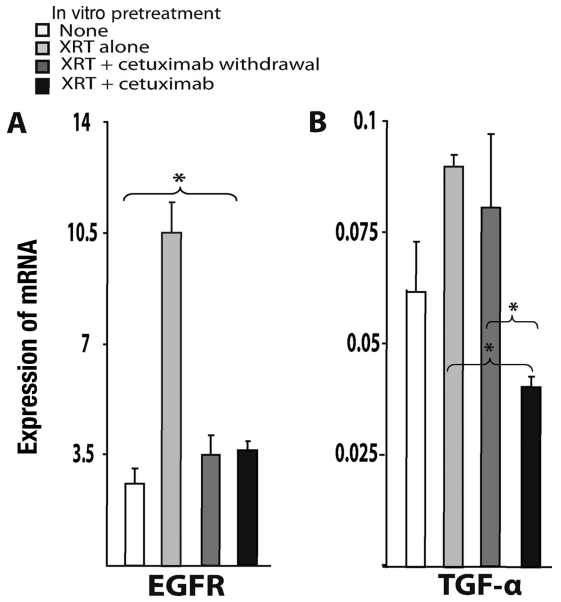

Figure 4. Radiation induced EGFR and TGF-α mRNA expression and cetuximab inhibited it. At day corresponding to A431 cell implantation, quantification of mRNA was performed as described in Materials and Methods. Values are the mean ± standard error of three independent experiments with two replicates per experiment.

*$p < .05$ (Mann-Whitney test).

Abbreviations: EGFR, epidermal growth factor receptor; TGF-α, transforming growth factor α; XRT, radiation.

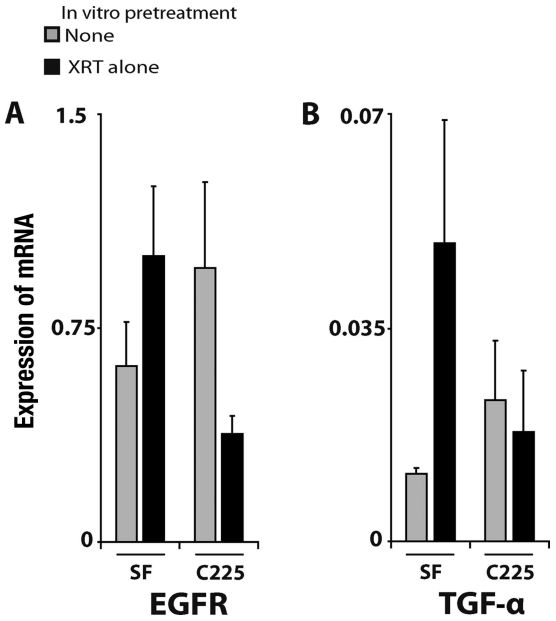

Figure 5. Expression of EGFR and TGF-α mRNA induced by in vitro XRT was maintained in xenografts, where it was subsequently blocked by cetuximab. Quantification of mRNA was carried out as described in Materials and Methods. Values are the mean ± standard error of three independent experiments with three tumors measured per duplicate per experiment.

Abbreviations: EGFR, epidermal growth factor receptor; TGF-α, transforming growth factor α; XRT, radiation.

these cells had a low baseline MVD that was not significantly reduced further by exposure to cetuximab in vivo.

Finally, because ionizing radiation was found to be associated with greater MVD, we examined whether the release of the main endothelial mitogenic factor (VEGF) was stimulated by radiation. VEGF supernatant levels in cell cultures increased progressively, such that within 48 hours after irradiation they were more than double the control values (2.82×). In addition, we demonstrated that treatment with cetuximab inhibited this VEGF secretion (supplemental online Fig. S3).

Our experimental data strongly suggest that fractionated ionizing radiation promotes biological changes in A431 cells, including activation of the EGFR and VEGF pathways, which may have orchestrated a cytoprotective response to prepare cells for survival, resulting in the observed malignant phenotype.

Discussion

In this study, we evaluated maintenance anti-EGFR therapy, specifically cetuximab treatment, in reducing recurrences after radiotherapy in a preclinical setting. At present, this topic has important implications in patient management, and several preclinical studies and clinical trials have been undertaken to elucidate answers to this question [9, 18]. The main accomplishment of our study was to demonstrate the feasibility of using an EGFR antibody to inhibit the progression of a subpopulation of A431 cells that survived a biologically significant dose of radiation, as likely occurs in residual disease. This cell subpopulation originated tumors with a more aggressive phenotype, as evidenced by a higher growth rate and greater angiogenesis. This phenotype was associated with activation of EGFR signaling and VEGF expression. Cetuximab was effective in inhibiting tumor growth after radiation and partially blocked EGFR signaling both in vivo and in vitro. Our findings provide evidence to support the clinical evaluation of maintaining cetuximab treatment after radiotherapy, wherein it could play a role in controlling EGFR-activated and relatively more radioresistant clones.

Treatment with cetuximab delayed tumor growth in all settings analyzed, including tumors originating from previously irradiated cells showing a more aggressive behavior. Radiation-induced phenotypes similar to those we found have been described previously [19, 20] and cancer stem cells with comparable properties have also been reported [21, 22]. Irradiated cells are known to have the ability to activate cytoprotective mechanisms as an adaptive response to the cell-killing effects of radiation; once these mecha-

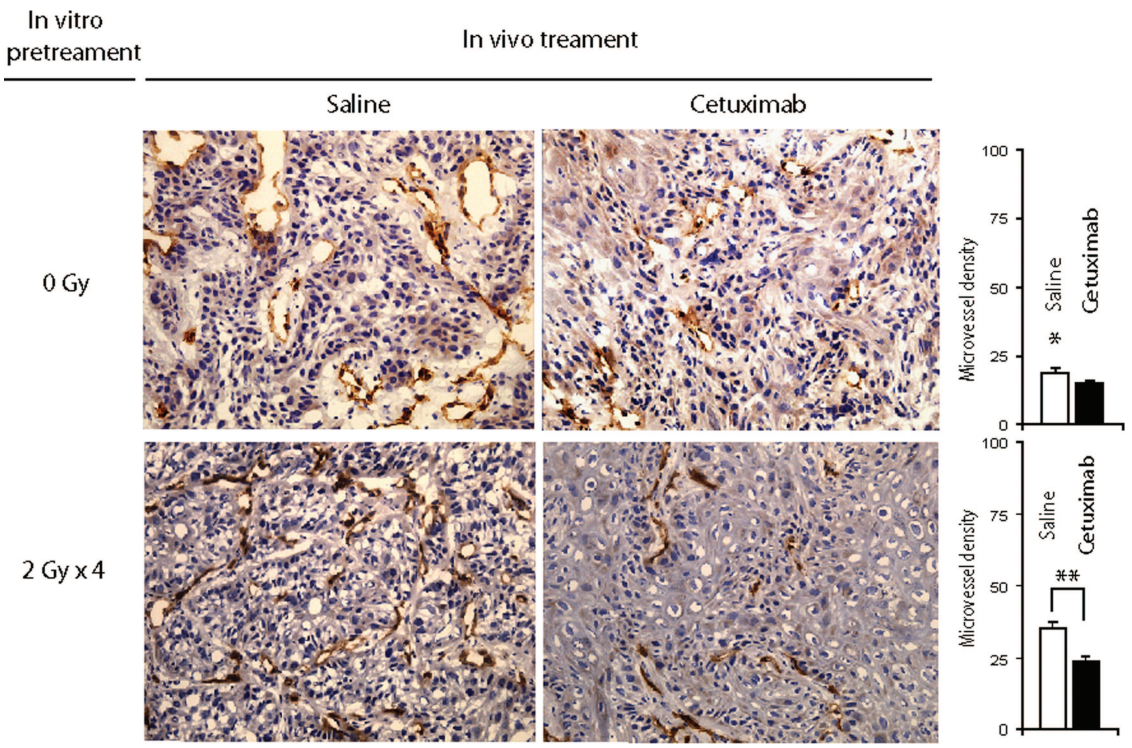

Figure 6. Cetuximab preferentially inhibited angiogenesis in tumors arising from in vitro–irradiated A431 cells. Illustrative CD31 (platelet and endothelial cell adhesion molecule 1) immunostainings (40×) of xenografted tumors are depicted.
*$p < .05$, compared with tumors derived from irradiated cells in saline-treated mice.
**$p < .0001$ (Student's t-test).

nisms have been triggered, radiotherapy treatment may be unsuccessful. Failures resulting from protracted radiotherapy have been associated with radiation-induced accelerated tumor growth [23]. Ionizing radiation is known to induce radiation-induced ligand-independent activation of EGFR, phosphorylation of members of the Src family, and VEGF overexpression [23–25]. In the experimental model we used to mimic residual disease, we found that the ERK-1/2 and Akt kinases downstream of EGFR were persistently activated in response to radiation. Also, cells surviving after radiotherapy displayed higher levels of EGFR and TGF-α mRNA both in vivo and in vitro. Likewise, tumors derived from these cells had greater MVD, likely dependent on greater VEGF secretion. Iterating irradiation primed, in our experimental design, a subpopulation of relatively radioresistant cells that not only retains cancer stem cell properties—such as clonogenicity and tumor-initiating ability—but also exhibits more aggressive traits, qualities often attributed to microscopic residual disease. Furthermore, once this subpopulation of EGFR-activated surviving cells became addicted to this signaling pathway, it may have been rendered more susceptible to cetuximab than unirradiated cells.

Cetuximab maintenance treatment partially reverted the greater EGFR/TGF-α expression observed in irradiated cells both in vitro and in vivo, as well as the VEGF secretion and greater MVD. In spite of this partial blockade, no significant differences were observed between the in vitro pretreatment schedules regarding the efficacy of cetuximab. The discrepancy between EGFR targeting and efficacy suggests that EGFR addiction is unlikely to account fully for the phenotype associated with radiation. Other factors may have contributed to this discrepancy, including the activation of other signaling pathways in response to radiation, transient adaptation to cetuximab exposure (Fig. 1), the relative lack of knowledge of cetuximab pharmacokinetics in mice, the potential effect of stroma on tumor cell behavior, and the difficulty of estimating the influence of the retrieval cetuximab prior to in vivo implantation. Finally, we did not find evidence of an ADCC mechanism of action.

In addition to inhibiting tumor progression, treatment with cetuximab decreased vascularization at an early stage. Huang and Harari also found an association between delayed tumor growth and reduction of microvessels in irradiated mice treated with high doses of radiation (18 Gy, single fraction) and cetuximab [26]. However, because the tumors were irradiated in those experiments, delayed cell growth and microvessel reduction might have been caused by the direct effects of radiation cytotoxicity on endothelial cells or by downregulation of vascular growth factors [17,

27]. In contrast, tumor xenografts in our model were not irradiated, so a primary effect of radiation on host stromal and endothelial cells can be ruled out. Furthermore, we found that radiation induced VEGF secretion, a response consistent with a biological mechanism to protect cells from the lethal effects of radiation. Similar findings in response to radiation were described previously in Lewis lung carcinoma cells [25]. Thus, it seems reasonable to conclude that our results indicate that radiation activated the EGFR signaling cascade, upregulating the synthesis of prosurvival substances—including VEGF. This could explain the high MVD we found in xenografts, probably to support cancer cell survival and tumor progression. Because mouse cells are not recognized by cetuximab, it is clear that the reduced MVD observed in cetuximab-treated mice must have originated as a consequence of blocking EGFR in A431 cells.

Although cetuximab clearly inhibited irradiated A431 cells, our data raise concerns about resistance to cetuximab. The obvious antitumor effect of cetuximab is in sharp contrast to the cell desensitization to cetuximab that developed in vitro. Whereas the MVD value depended on in vitro and in vivo cetuximab treatment in smaller tumors, this association disappeared in large tumors (data not shown), suggesting that cells can eventually evade the initial antiangiogenic action. Such considerations and the lack of cetuximab antitumor efficacy in in vitro pretreatments may warrant more preclinical studies to evaluate combinations of cetuximab and other agents that target cell survival pathways to overcome treatment resistance, not only as a systemic therapy but also in association with radiotherapy.

The main data from this study come from only one cell line, and therefore caution should be taken in interpreting them in clinical practice. However, the fact that two different carcinoma cells, which differ in origin and in EGFR expression level, reacted similarly to radiation by increasing the activity of the relevant kinases indicates that the mechanisms described here could actually be shared by other carcinoma cells as well. Finally, we believe that our preclinical results may help to understand the mechanisms underlying cetuximab treatment after radiotherapy.

In conclusion, our experimental findings suggest that tumor cells that survive radiotherapy express a radiation-induced cytoprotective phenotype that is susceptible to inhibition through additional treatment with an anti-EGFR antibody. In our opinion, these findings have clinical relevance and provide further support for carrying out clinical trials to examine the use of maintenance cetuximab after radiotherapy to increase curability and prolong the disease-free interval in patients with tumors that are dependent on EGFR.

ACKOWLEDGMENTS

We are grateful to Bradley J. Londres for his excellent assistance in improving the English in the manuscript.

We thank Merck-Serono Spain for its financial support.

AUTHOR CONTRIBUTIONS

Conception/Design: Gemma Pueyo, Ricardo Mesia, Alicia Lozano, Silvia-Vazquez, Gabriel Capella, Josep Balart
Provision of study material or patients: Gemma Pueyo, Agnes Figueras, Marta Baro, Josep Balart
Collection and/or assembly of data: Gemma Pueyo, Josep Balart
Data analysis and interpretation: Gemma Pueyo, Ricardo Mesia, Agnes Figueras, Alicia Lozano, Marta Baro, Silvia Vazquez, Gabriel Capella, Josep Balart
Manuscript writing: Gemma Pueyo, Ricardo Mesia, Gabriel Capella, Josep-Balart
Final approval of manuscript: Josep Balart

REFERENCES

1 Phillips TM, McBride WH, Pajonk F. The response of CD24(-/low)/CD44+ breast cancer-initiating cells to radiation. J Natl Cancer Inst 2006;98:1777–1785.

2 Keith B, Simon MC. Hypoxia-inducible factors, stem cells, and cancer. Cell 2007;129:465–472.

3 Bartkova J, Horejsi Z, Koed K et al. DNA damage response as a candidate anti-cancer barrier in early human tumorigenesis. Nature 2005;434:864–870.

4 Abbott A. Cancer: The root of the problem. Nature 2006;442:742–743.

5 Rich JN. Cancer stem cells in radiation resistance. Cancer Res 2007;67:8980–8984.

6 Jorissen RN, Walker F, Pouliot N et al. Epidermal growth factor receptor: Mechanisms of activation and signalling. Exp Cell Res 2003;284:31–53.

7 Liang K, Ang KK, Milas L et al. The epidermal growth factor receptor mediates radioresistance. Int J Radiat Oncol Biol Phys 2003;57:246–254.

8 Bonner JA, Harari PM, Giralt J et al. Radiotherapy plus cetuximab for squamous-cell carcinoma of the head and neck. N Engl J Med 2006;354:567–578.

9 Milas L, Fang FM, Mason KA et al. Importance of maintenance therapy in C225-induced enhancement of tumor control by fractionated radiation. Int J Radiat Oncol Biol Phys 2007;67:568–572.

10 Vermorken JB, Mesia R, Rivera F et al. Platinum-based chemotherapy plus cetuximab in head and neck cancer. N Engl J Med 2008;359:1116–1127.

11 Weidner N, Semple JP, Welch WR et al. Tumor angiogenesis and metastasis—correlation in invasive breast carcinoma. N Engl J Med 1991;324:1–8.

12 Viloria-Petit AM, Kerbel RS. Acquired resistance to EGFR inhibitors: Mechanisms and prevention strategies. Int J Radiat Oncol Biol Phys 2004;58:914–926.

13 Lu Y, Li X, Liang K et al. Epidermal growth factor receptor (EGFR) ubiquitination as a mechanism of acquired resistance escaping treatment by the anti-EGFR monoclonal antibody cetuximab. Cancer Res 2007;67:8240–8247.

14 Wolterink S, Moldenhauer G, Fogel M et al. Therapeutic antibodies to hu-

man L1CAM: Functional characterization and application in a mouse model for ovarian carcinoma. Cancer Res 2010;70:2504–2515.

15 Nasu S, Ang KK, Fan Z et al. C225 antiepidermal growth factor receptor antibody enhances tumor radiocurability. Int J Radiat Oncol Biol Phys 2001;51:474–477.

16 Song JY, Lee SW, Hong JP et al. Epidermal growth factor competes with EGF receptor inhibitors to induce cell death in EGFR-overexpressing tumor cells. Cancer Lett 2009;283:135–142.

17 Perrotte P, Matsumoto T, Inoue K et al. Anti-epidermal growth factor receptor antibody C225 inhibits angiogenesis in human transitional cell carcinoma growing orthotopically in nude mice. Clin Cancer Res 1999;5:257–265.

18 Mesia R, Rueda A, Vera R et al. Safety report of a randomized phase II trial to evaluate the combination of cetuximab plus accelerated concomitant boost radiotherapy (RT) followed or not by cetuximab monotherapy in patients (pts) with locally advanced squamous cell carcinoma of the oropharynx. J Clin Oncol 2008;26(suppl 15):6076.

19 Schmidt-Ullrich RK, Mikkelsen RB, Dent P et al. Radiation-induced proliferation of the human a431 squamous carcinoma cells is dependent on EGFR tyrosine phosphorylation. Oncogene 1997;15:1191–1197.

20 Bozec A, Sudaka A, Fischel JL et al. Combined effects of bevacizumab with erlotinib and irradiation: A preclinical study on a head and neck cancer orthotopic model. Br J Cancer 2008;99:93–99.

21 Bao S, Wu Q, Sathornsumetee S et al. Stem cell-like glioma cells promote tumor angiogenesis through vascular endothelial growth factor. Cancer Res 2006;66:7843–7848.

22 Bao S, Wu Q, McLendon RE et al. Glioma stem cells promote radioresistance by preferential activation of the DNA damage response. Nature 2006; 444:756–760.

23 Schmidt-Ullrich RK. Molecular targets in radiation oncology. Oncogene 2003;22:5730–5733.

24 Kharbanda S, Yuan ZM, Rubin E et al. Activation of Src-like p56/p53lyn tyrosine kinase by ionizing radiation. J Biol Chem 1994;269:20739–20743.

25 Gorski DH, Beckett MA, Jaskowiak NT et al. Blockage of the vascular endothelial growth factor stress response increases the antitumor effects of ionizing radiation. Cancer Res 1999;59:3374–3378.

26 Huang SM, Harari PM. Modulation of radiation response after epidermal growth factor receptor blockade in squamous cell carcinomas: Inhibition of damage repair, cell cycle kinetics, and tumor angiogenesis. Clin Cancer Res 2000;6:2166–2174.

27 Lichter AS, Lawrence TS. Recent advances in radiation oncology. N Engl J Med 1995;332:371–379.